A&A 482, 333–340 (2008)
DOI: 10.1051/0004-6361:20079062

Astronomy & Astrophysics

Constraints on resonant-trapping for two planets embedded in a protoplanetary disc

A. Pierens and R. P. Nelson

Astronomy Unit, Queen Mary, University of London, Mile End Rd, London, E1 4NS, UK
e-mail: a.pierens@qmul.ac.uk

Received 13 November 2007 / Accepted 13 February 2008

ABSTRACT

Context. A number of extrasolar planet systems contain pairs of Jupiter-like planets in mean motion resonances. As yet there are no known resonant systems which consist of a giant planet and a significantly lower-mass body.
Aims. We investigate the evolution of two-planet systems embedded in a protoplanetary disc, which are composed of a Jupiter-mass planet plus another body located further out in the disc. The aim is to examine how the long-term evolution of such a system depends on the mass of the outer planet.
Methods. We have performed 2D numerical simulations using a grid-based hydrodynamics code. The planets can interact with each other and with the disc in which they are embedded. We consider outermost planets with masses ranging from 10 $M_\oplus$ to 1 M_J. Combining the results of these calculations and analytical estimates, we also examine the case of outermost bodies with masses $<10\ M_\oplus$.
Results. Differential migration of the planets due to disc torques leads to different evolution outcomes depending on the mass of the outer protoplanet. For planets with mass $\lesssim 3.5\ M_\oplus$ the type II migration rate of the giant exceeds the type I migration rate of the outer body, resulting in divergent migration. Outer bodies with masses in the range $3.5 < m_\mathrm{o} \leq 20\ M_\oplus$ become trapped at the edge of the gap formed by the giant planet, because of corotation torques. Higher mass planets are captured into resonance with the inner planet. If $30 \leq m_\mathrm{o} \leq 40\ M_\oplus$ or $m_\mathrm{o} = 1\ M_\mathrm{J}$, then the 2:1 resonance is established. If $80 \leq m_\mathrm{o} \leq 100\ M_\oplus$, the 3:2 resonance is favoured.
Simulations of gas-accreting protoplanets of mass $m_\mathrm{o} \geq 20\ M_\oplus$, trapped initially at the edge of the gap, or in the 2:1 resonance, also result in eventual capture in the 3:2 resonance as the planet mass grows to become close to the Saturnian value.
Conclusions. Our results suggest that there is a theoretical lower limit to the mass of an outer planet that can be captured into resonance with an inner Jovian planet, which is relevant to observations of extrasolar multiplanet systems. Furthermore, capture of a Saturn-like planet into the 3:2 resonance with a Jupiter-like planet is a very robust outcome of simulations, independent of initial conditions. This result is relevant to recent scenarios of early Solar System evolution which require Saturn to have existed interior to the 2:1 resonance with Jupiter prior to the onset of the Late Heavy Bombardment.

Key words. accretion, accretion disks – planetary systems: formation – hydrodynamics – methods: numerical

1. Introduction

To date, about 25 extrasolar multiplanet systems have been discovered (e.g. http://exoplanet.eu/). Interestingly, at least 5 of them contain two planets trapped in a low-order mean motion resonance. For example, the planets in GJ 876, HD 128311, HD 82943, HD 73526 appear to be in 2:1 resonance while two of the four planets orbiting in the 55 Cnc system are in 3:1 resonance.

The existence of resonant systems can be understood by a model in which two planets undergo differential migration, due to their interaction with a protoplanetary disc, and become locked in the resonance as their orbits converge. This scenario has been explored by numerous hydrodynamic simulations of two embedded giant planets interacting with each other and undergoing type II migration (Snellgrove et al. 2001; Papaloizou 2003; Kley et al. 2004, 2005), and also by N-body simulations with prescribed forces designed to mimic disc torques (Snellgrove et al. 2001; Lee & Peale 2002; Nelson & Papaloizou 2002). The evolution of such a system generally proceeds as follows. Because giant planets are able to open a gap in the disc, there is a tendency for the gaseous material between them to be cleared, leading ultimately to a two-planet system orbiting within a common gap. From this time onward, the migration of the system is such that the planets are on converging orbits. The final outcome is generally found to be trapping into 2:1 resonance, which corresponds to the most common resonance observed in extrasolar systems.

Masset & Snellgrove (2001) investigated the particular case where the inner planet has a Jupiter mass but where the mass of the outer planet is characteristic of that of Saturn. In that case, Saturn tends to undergo a fast runaway migration (Masset & Papaloizou 2003) and rapidly catches up with Jupiter, which drifts inward much more slowly. Because their orbits converge quickly, Saturn passes through the 2:1 resonance with Jupiter but becomes captured into the 3:2 resonance. These results were confirmed by Morbidelli & Crida (2007) who examined the same problem, but considered a larger range of initial parameters using a code that describes more accurately the global viscous evolution of the disc.

So far, there have been few studies focused on the interaction between a Jupiter-mass planet and a protoplanetary core with significantly lower mass (e.g. $\sim 10\ M_\oplus$). As a result of disc

torques, low-mass planets are known to undergo rapid inward migration (so-called type I migration) (Ward 1997; Tanaka et al. 2002). For typical disc parameters, the type I migration time scale of a protoplanet with mass 10 $M_\oplus$ is a few $\times 10^4$ years, which is significantly shorter than the type II migration time scale (usually quoted as being $\sim 10^5$ years). Therefore, a sufficiently massive body undergoing type I migration can eventually become captured into resonance with a giant planet located inside its orbit (Hahn & Ward 1996). Using N-body simulations, Thommes (2005) recently focused on the evolution of such a two-planet system. He showed that indeed, bodies of Earth to Neptune-mass size have a high likelihood of being captured in the exterior mean motion resonances of the giant. In this work, the disc torques are modelled as prescribed forces using classical analytical expressions for the migration and eccentricity damping rates (Papaloizou & Larwood 2000). Although the effects of Lindblad torques are well captured by such an approach, the corotation torques acting on the low-mass planet are neglected. However, as the latter approaches the edge of the gap opened by Jupiter, where the disc surface density gradient is large and positive, corotation torques can become dominant and significantly change the dynamics of the system. As shown by Masset et al. (2006), type I migration can eventually be halted in a region of the disc with a strongly positive surface density gradient. Migration-halting arises once the protoplanet reaches a fixed point where the corotation torques, which are positive near the gap edge, exactly counterbalance the negative Lindblad torques. In this paper we examine how this affects the capture into resonance of low mass outer planets by an interior giant planet.

We present the results of hydrodynamical simulations of two-planet systems composed of a Jupiter-mass planet plus an outermost body whose mass can vary from 10 $M_\oplus$ to 1 M_J. We also consider the case of outermost bodies with masses $<10\ M_\oplus$ using the results of these simulations and analytical estimates. The aim of this work is to investigate how the evolution of such a system depends on the mass of the outer planet. In particular, we examine the issue of whether or not low-mass planets can become captured into resonance with an interior giant planet as a result of convergent migration. For the particular disc model we consider, the results of these simulations suggest that the final fate of the outermost body can be threefold: (i) protoplanets with masses $\lesssim 3.5\ M_\oplus$ undergo type I migration at a slower rate than the type II migration experienced by the giant planet, so planetary configurations of this type experience divergent migration; (ii) protoplanets with masses of $3.5 < m_\mathrm{o} \leq 20\ M_\oplus$ become trapped at the edge of the gap formed by the inner giant due to corotation torques, where they remain over long time scales; (iii) higher mass bodies become captured into resonance with Jupiter. For planet masses in the range $30 \leq m_\mathrm{o} \leq 40\ M_\oplus$, or for $m_\mathrm{o} = 1\ M_\mathrm{J}$, capture is into the 2:1 resonance. For planet masses in the range $80 \leq m_\mathrm{o} \leq 100\ M_\oplus$, capture is into the 3:2 resonance. Interestingly, we find that trapping into 3:2 resonance is robust with respect to initial conditions of the outermost body, provided the disc is sufficiently massive. Indeed, simulations of a protoplanetary core initially trapped at the edge of the giant planet's gap, or in the 2:1 resonance, and accreting gas until its mass becomes characteristic of that of Saturn, resulted in eventual capture into the 3:2 resonance.

This paper is organized as follows. In Sect. 2 we describe the hydrodynamical model. In Sect. 3, we present the results of our simulations. In Sect. 4, we discuss out results within the context of the early history of the outer Solar System. We finally summarize and draw our conclusions in Sect. 5.

2. The hydrodynamical model

2.1. Numerical method

In this paper, we adopt a 2D disc model for which all the physical quantities are vertically averaged. We work in a non-rotating frame, and adopt cylindrical polar coordinates (r, ϕ) with the origin located at the position of the central star. Indirect terms resulting from the fact that this frame in non-intertial are incorporated in the equations governing the disc evolution (Nelson et al. 2000). These are solved using a hydrocode called GENESIS for which a full description can be found, for example, in De Val-Borro et al. (2006). The evolution of the planetary orbits is computed using a fifth-order Runge-Kutta integrator (Press et al. 1992). Here, all the planets and the disc can interact gravitationally with each other. The gravitational potential experienced by a planet from the disc is given by:

$$\Phi_\mathrm{d} = -G \int_S \frac{\Sigma(\boldsymbol{r}')\mathrm{d}\boldsymbol{r}'}{\sqrt{r'^2 + r_\mathrm{p}^2 - 2r' r_\mathrm{p}\cos(\phi' - \phi_\mathrm{p}) + \epsilon^2}} \tag{1}$$

where Σ is the disc surface density and where the integral is performed over the surface of the disc located outside the Hill sphere of the planet. r_p and ϕ_p are respectively the radial and azimutal coordinates of the planet. ϵ is smoothing length which is set to $\epsilon = 0.66\ H$, where H is the disc scale height at the planet orbit. We further note that we exclude the material contained in the planet Hill sphere when calculating this gravitational potential, since this material is gravitationally bound to the planet.

The computational units we adopt are such that the mass of the central star $M_\star = 1$ corresponds to one Solar mass, the gravitational constant is $G = 1$ and the radius $r = 1$ in the computational domain corresponds to 5 AU. In the following, time is measured in units of the orbital period at $r = 1$.

In the calculations presented here, we use $N_\mathrm{r} = 256$ radial grid cells uniformly distributed between $r_\mathrm{in} = 0.25$ and $r_\mathrm{out} = 5$ and $N_\phi = 380$ azimuthal grid cells.

2.2. Initial conditions

In the disc model employed for all the runs presented here, the disc aspect ratio is constant and equal to $H/r = 0.05$. We also adopt a locally isothermal equation of state for which the vertically integrated pressure P is given by:

$$P = c_\mathrm{s}^2 \Sigma. \tag{2}$$

In this equation, c_s is the local isothermal sound speed and can be written as:

$$c_\mathrm{s} = \frac{H}{r} v_\mathrm{K}, \tag{3}$$

where $v_\mathrm{K} = \sqrt{GM_\star/r}$ is the local Keplerian velocity. Using a locally isothermal equation of state implies that we do not evolve an energy equation in the work presented here. The initial disc surface density profile is chosen to be $\Sigma(r) = \Sigma_0\ r^{-1/2}$ where $\Sigma_0 = 6 \times 10^{-4}$ in dimensionless units. This gives a total initial disc mass within the computational domain $M_\mathrm{d} \sim 2 \times 10^{-2}\ M_\odot$. Furthermore, in order to model the anomalous viscous stress presumed to originate because of turbulence in the disc, we use the standard "alpha" prescription for the disc viscosity $\nu = \alpha c_\mathrm{s} H$ (Shakura & Sunyaev 1973), where c_s is the isothermal sound speed. In this work we set $\alpha = 10^{-3}$.

The inner and outermost planets initially evolve on circular orbits at $a_\mathrm{J} = 1$ and $a_\mathrm{o} = 2.2$ respectively. The mass of the inner

planet is $m_J = 1\ M_J$ and we consider outer planets with masses $m_o = 10$, 20, 30, 40, 80, 100 and 300 $M_\oplus$. In order to give the inner planet sufficient time to open a gap, we proceed in two steps:

i) we first consider a 30 $M_\oplus$ protoplanet held at $r = 1$ on a fixed circular orbit. This body is allowed to accrete gas from the disc on a dynamical time scale until its mass reaches 1 M_J. Such an approach is fairly consistent with evolutionary models of gas giant planets forming in protoplanetary discs which suggest that rapid gas accretion occurs once the planet mass exceeds 30−40 $M_\oplus$ (Papaloizou & Nelson 2005).
ii) we restart this model, but with an additional outer body located at $r = 2.2$. If the mass of latter exceeds 30 $M_\oplus$, we adopt the procedure described in i) above in order to obtain the relevant value for m_o. We then release both planets and let them evolve under the action of disc torques.

2.3. Boundary conditions

At the inner edge of the computational domain, we model the accretion onto the central star by setting the radial velocity in the innermost cells to $v_r(r_{in}) = \beta\ v_{visc}(r_{in})$, where $v_{visc}(r_{in}) = -3\nu/2r_{in}$ is the typical inward drift velocity for a steady-state accretion disc, and β is a free parameter. Contrary to the standard open boundary conditions which are commonly used in hydrodynamical simulations, these boundary conditions prevent the inner disc from emptying too quickly. In order to find a suitable value for β, we performed a series of test simulations of an embedded Jupiter-mass planet, and varied the value for β. We then compared the final state of these calculations to the results of simulations performed by Crida et al. (2007), in which the global disc evolution is more accurately modelled. Although the value for β might be problem-dependant, choosing $\beta = 5$ gives good agreement with the results obtained by Crida et al. (2007) for our particular setup. We therefore adopt this value in the simulations presented here. We also use linear viscosity between the inner boundary and $r = 0.45$ to prevent wave reflection (Stone & Norman 1992).

In order to avoid any wave reflection at the outer edge of the computational domain, we employ a wave killing zone in the vicinity of the outer boundary, in which we solve the following equation at each time step (De Val-Borro et al. 2006):

$$\frac{dX}{dt} = -\frac{X - X_0}{\tau} R(r). \quad (4)$$

In the previous equation, X represents either the surface density or one of the velocity components and X_0 is the initial value of the correponding quantity. τ is the orbital period at the outer boundary, and $R(r)$ is a quadratic function which varies from $R(4) = 0$ to $R(5) = 1$. At the outer edge of the computational domain, the radial velocity is set to zero, preventing thereby inflow/outflow of matter there.

3. Results

For each value of m_o we consider, we have performed a simulation in which the evolution of the system was followed for a run time of $\sim 10^4$ orbits at $r = 1$. The results of the simulations are shown in Table 1. These indicate that, depending on the value of m_o, the evolution of the system can take three different paths: divergent migration, such that the inner planet migrates inward faster than the outer planet; trapping of the outer planet at the edge of the gap opened by the giant planet; capture of the outer planet into a mean motion resonance with the inner giant. We describe in detail these three different modes of evolution in the following sections.

Table 1. The first column gives the run label, the second column gives the mass m_o of the outer planet and the third column gives the state of the system at the end of the simulation.

Model	m_o ($M_\oplus$)	Result
R1	10	Trapping at the edge of gap
R2	20	Trapping at the edge of gap
R3	30	2:1 resonance
R4	40	2:1 resonance
R5	80	3:2 resonance
R6	100	3:2 resonance
R7	300	2:1 resonance

3.1. Divergent migration

Although we have not explicitly simulated the evolution of an inner giant planet with an outer planet whose mass is less than 10 $M_\oplus$, we can see from Fig. 1 that the typical specific torque experienced by the giant planet, once gap formation is complete, is $\sim 9 \times 10^{-6}$. Early on in the evolution of the 10 $M_\oplus$ planet, we see that the total specific torque is $\sim 1.8 \times 10^{-5}$. Given that the migration rate of a planet is related to the specific torque T_p by:

$$\frac{dr_p}{dt} = 2\sqrt{\frac{GM_\star}{r_p}} T_p, \quad (5)$$

and the initial location of the Jovian mass planet is $r_p = 1$ whereas that of the 10 $M_\oplus$ body is $r_p = 2.2$, we estimate that a planet of mass $\sim 3.5\ M_\oplus$ will migrate at the same rate as the giant. This suggests that an outer planet of mass $\lesssim 3.5\ M_\oplus$ will not be able to catch up with the migrating giant, and the long term evolution will involve divergent migration.

3.2. Trapping at the edge of the gap

Simulations in which $m_o = 10\ M_\oplus$ (model R1) or $m_o = 20\ M_\oplus$ (model R2) resulted in the outer planet being trapped at the outer edge of the giant's tidally maintained gap. The time evolution of the planets' semi-major axes for both models is shown in the upper panel of Fig. 1. In these runs, the evolution of the system proceeds as follows. At the beginning of the simulation, each body migrates inward as a result of disc torques. However, as illustrated by the lower panels of Fig. 1 which display the evolution of the specific torques acting on the planets, the type I migration of the outer planet tends to be faster than the type II migration of the giant. The two planets converge as a result of this differential migration, as illustrated by a decrease in their period ratio $p = (a_o/a_J)^{1.5}$, whose evolution is depicted in the middle panel of Fig. 1. We see that after an initial period of decrease, the period ratio then increases for both models. This occurs from $t \sim 2 \times 10^3$ orbits for run $R1$, and from $t \sim 4 \times 10^3$ orbits for simulation $R2$. Subsequently, the period ratio decreases again and is likely to enter a sequence of cyclic variations as the outer planets oscillate around the fixed points where their corotation and Lindblad torques counterbalance. This phenomenon is triggered once the outermost planet reaches the edge of the gap opened by the inner giant, and suggests that such planets are unable to approach any closer to the giant, but instead remain trapped near the gap edge.

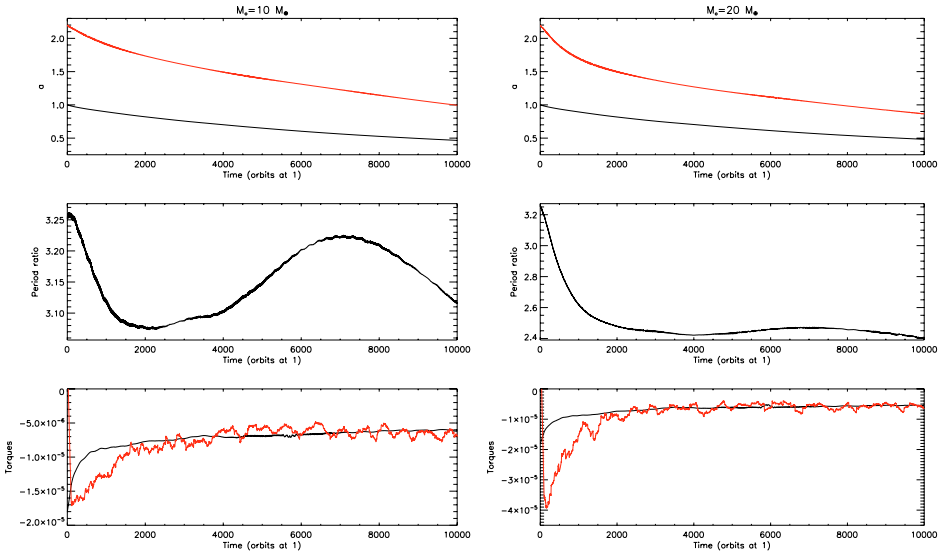

Fig. 1. This figure shows the evolution of the system for models $R1$ (*left panel*) and $R2$ (*right panel*). In both cases, the giant planet is represented by black line and the outer planet is represented by red line. *Top*: evolution of the semi-major axes for both planets. *Middle*: evolution of the period ratio $p = (a_o/a_J)^{1.5}$. *Bottom*: evolution of the disc torques acting on the planets.

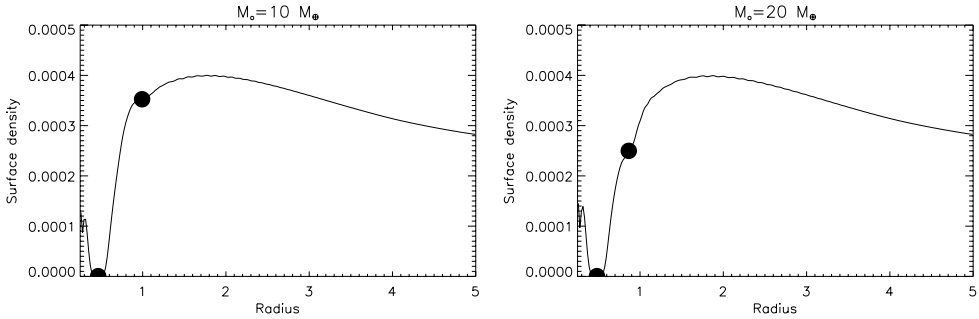

Fig. 2. This figure shows the surface density profile for runs $R1$ (*left panel*) and $R2$ (*right panel*) at $t \sim 10^4$. In this figure, the planets are represented by black circles.

For model $R1$ (model $R2$), the disc surface density profile after $\sim 10^4$ orbits is represented on the left (right) panel of Fig. 2. Clearly, the outer planet is located in a region of strong positive surface density gradient, where the corotation torque is positive and can eventually counterbalance the negative differential Lindblad torque (Masset et al. 2006). In comparison with the 10 $M_\oplus$ planet, we see that the migration of the 20 $M_\oplus$ body is halted closer to the giant, in a region where the disc specific vorticity (vortensity) gradient is larger. This arises because the specific corotation torque scales linearly with planet mass for low mass bodies ($m_p \leq 10\ M_\oplus$) whereas it scales with $m_p^{1/3}$ for $m_p > 50\ M_\oplus$. For planets in between these masses, the exponent lies in the range $1-1/3$ (Masset et al. 2006). Therefore, a 20 $M_\oplus$ planet requires a steeper vortensity gradient than a 10 $M_\oplus$ body to counterbalance the Lindblad torques.

Interestingly, examination of the disc torques which are represented in the lower panel of Fig. 1 reveals that once the outer planet is trapped, the total specific torque exerted on the latter oscillates around a mean value corresponding to the specific torque acting on the giant. This indicates that the outermost planet tends to follow the evolution of the gap edge due to the migration of the giant. This phenomenon is in good agreement with the simulations performed by Masset et al. (2006) which showed a 15 $M_\oplus$ planet remaining trapped at the edge of an expanding cavity.

It is well known that corotation torques can saturate in the absence of viscosity or some other dissipative mechanism that is able to maintain the surface density gradient in the vicinity of the planet (Ogilvie & Lubow 2003; Masset et al. 2006). Here, the simulations cover a run time which greatly exceeds the horseshoe libration time scale, and show no evidence for corotation torque saturation. In this paper, the viscous parameter is $\alpha = 10^{-3}$, which is large enough to prevent the corotation torque saturation for planet masses between 10–20 $M_\oplus$ (Masset et al. 2006).

3.3. Capture in mean motion resonance

3.3.1. Models R3 and R4

For calculations with $m_o \geq 30\ M_\oplus$, we find that the outer planet can migrate through the gap region and stable mean motion resonances are formed between the inner giant and the outermost body. The two upper panels in Fig. 3 show the evolution of the semi-major axes and eccentricities of the planets for models $R3$ and $R4$. In model $R3$, the mass of the outer planet is $m_o = 30\ M_\oplus$ while it is $m_o = 40\ M_\oplus$ in model $R4$. Here again, the outer planet migrates faster initially and catches up with the inner body. In both cases, we find that the convergence of orbits subsequently leads to the formation of a 2:1 resonance between the two planets. Resonant capture occurs at $t \sim 2 \times 10^3$ orbits for model $R3$, and at the earlier time of $\sim 1.5 \times 10^3$ orbits for model $R4$. The lower panel of Fig. 3 displays the time evolution of the resonant

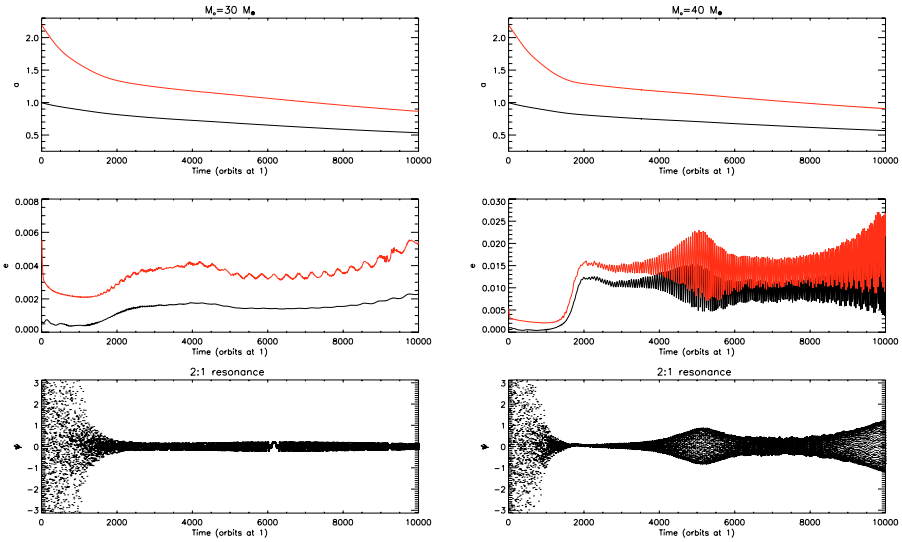

Fig. 3. This figure shows the evolution of the system for models $R3$ (*left panel*) and $R4$ (*right panel*). In both cases, the giant is represented by black line and the outer planet is represented by red line. *Top*: evolution of the semi-major axes for both planets. *Middle*: evolution of the planets' eccentricities. *Bottom*: evolution of the resonant angle $\psi = 2\lambda_o - \lambda_J - \varpi_J$ associated with the 2:1 resonance.

angle $\psi = 2\lambda_o - \lambda_J - \varpi_J$ associated with the 2:1 resonance, where λ_J (λ_o) and ϖ_J are respectively the mean longitude and longitude of pericentre of the innermost (outermost) planet. We see that ψ undergoes libration with a smaller amplitude in run $R3$, which indicates that the planets are locked deeper in the resonance in that case. Subsequent to this resonant capture, the continued evolution of the system in both models is such that the two planets migrate inward together while maintaining the commensurability.

Figure 4 displays, for model $R4$, the evolution of the disc torques exerted on both the Jovian mass planet and the 40 $M_\oplus$ body. Comparing this figure with Fig. 1, we see that for model $R4$, the torques exerted on the outermost body differ significantly to the ones exerted on the giant planet. This indicates that two planets locked in resonance exchange angular momentum in order for them to migrate at the same rate, which is not the case of the planets in models $R1$ and $R2$.

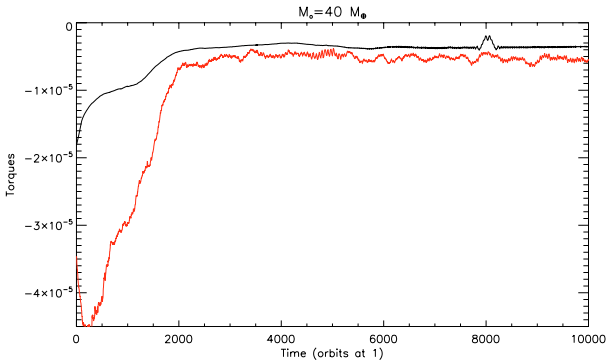

Fig. 4. This figure shows, for model $R4$, the evolution of the disc torques exerted on the giant planet (black line) and on the 40 $M_\oplus$ planet (red line).

3.3.2. Models R5 and R6

The evolution of the semi-major axes and eccentricities of the planets for models $R5$ and $R6$ are displayed in the two upper panels of Fig. 5. The mass of the outer planet in model $R5$ is $m_o = 80\ M_\oplus$ whereas it is $m_o = 100\ M_\oplus$ in model $R6$, which is characteristic of Saturn's mass. In both models, the outermost planet initially migrates in very rapidly as it undergoes runaway migration (Masset & Papaloizou 2003). In run $R5$, the 80 $M_\oplus$ planet reaches the location of the 2:1 resonance with Jupiter at $t \sim 10^3$ orbits where it remains temporarily captured, before slipping through into the 3:2 resonance at $t \sim 4 \times 10^4$ orbits. In run $R6$, the evolution of the Saturn-mass planet is similar, although it passes though the 2:1 resonance without being trapped. The evolution of the resonant angle $\psi = 3\lambda_o - 2\lambda_J - \varpi_J$ associated with the 3:2 resonance is presented, for both models, in the lower panel of Fig. 5.

In agreement with Masset & Snellgrove (2001) who were the first to examine the dynamics of a Jupiter plus Saturn system embedded in a protoplanetary disc, we find that the evolution outcome is such that the two planets migrate outward together maintaining the 3:2 resonance. Outward migration is favoured because the planets tend to share a common gap as they approach each other. Since Lindblad torques scale as $\sim m_p^2$, the positive torques exerted by the inner disc on Jupiter are larger than the negative torques acting on the outermost planet, thereby resulting in the outward migration of the system (Masset & Snellgrove 2001). Such a process can be maintained because there is a permanent flow of disc material from the outer disc across the gap. This can be seen in Fig. 6 which displays the disc surface density profile for model $R6$ at different times. Clearly, the inner disc surface density increases as the planets migrate outward. As noted by Masset & Snellgrove (2001), the mass flow across the gap has two important effects which enable the outward migration to be sustained. First, it continuously supplies the inner disc with gas, thereby maintaining a large value for the inner disc torques. Second, the gas flowing through the gap exerts positive corotation torques on the planets, although Morbidelli & Crida (2007) have recently shown that their consequence for the evolution of the system is sub-dominant compared with the positive inner disc torques.

It is worth noting that the reversed migration of the planets may depend on both the numerical and physical parameters involved. Morbidelli & Crida (2007) recently performed simulations of the same system and examined how the evolution outcome depends on initial conditions and disc parameters. They

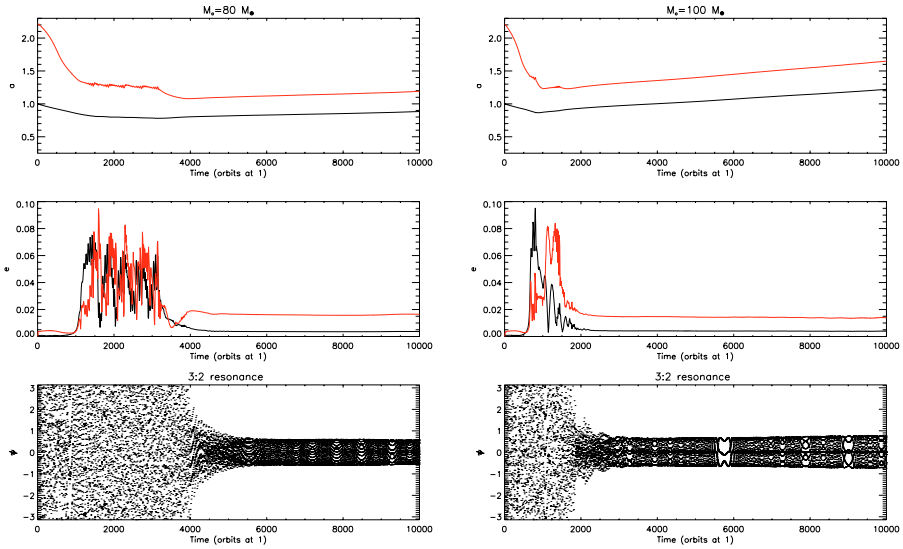

Fig. 5. This figure shows the evolution of the system for models *R*5 (*left panel*) and *R*6 (*right panel*). In both cases, the giant is represented by black line and the outer planet is represented by red line. *Top*: evolution of the semi-major axes for both planets. *Middle*: evolution of the planets' eccentricities. *Bottom*: evolution of the resonant angle $\psi = 3\lambda_o - 2\lambda_J - \varpi_J$ associated with the 3:2 resonance.

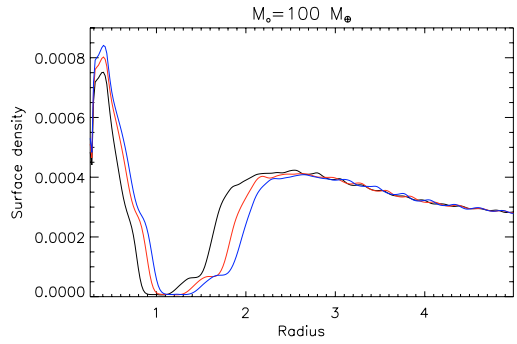

Fig. 6. This figure shows the disc surface density profile for model *R*6 at $t = 4 \times 10^3$ (black line), 8×10^3 (red line) and 10^4 (blue line) orbits.

have shown that although outward migration is robust with respect to numerical parameters, it is favoured in low viscosity and cool discs. In the simulations presented here, we adopted $\alpha = 10^{-3}$ which is clearly low enough for the outward migration to be maintained.

3.3.3. Model *R*7

The two upper panels of Fig. 7 show the evolution of the semi-major axes and eccentricities of the planets for model *R*7. Here, $m_o = 1\ M_J$ so that both the inner and outermost planets undergo slow type II migration initially. At $t \sim 800$ orbits the migration of the innermost planet is reversed, leading to convergence of the planet orbits. This occurs because the gas located between the two planets tends to be cleared as the gaps formed by them join together. The inner planet is then positively torqued by the inner disc, but experiences a reduced negative torque from the outer disc, causing its direction of migration to reverse. This effect is compounded by the fact that some of the gas originally located between the planets flows through into the inner disc, augmenting the positive torque it exerts. This can be seen clearly in the upper panel of Fig. 8 which displays the disc surface density profile at different times from the beginning of the two-planet evolution. The convergent migration causes the two planets to become locked in the 2:1 resonance at $t \sim 1.5 \times 10^3$ orbits. The

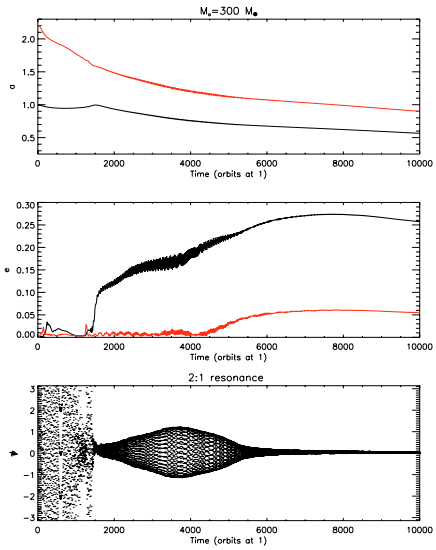

Fig. 7. This figure shows the evolution of the system for model *R*8. *Top*: evolution of the semi-major axes for both planets. *Middle*: evolution of the planets' eccentricities. *Bottom*: evolution of the resonant angle $\psi = 2\lambda_o - \lambda_J - \varpi_J$ associated with the 2:1 resonance.

time evolution of the resonant angle $\psi = 2\lambda_o - \lambda_J - \varpi_J$ associated with the 2:1 resonance is presented in the lower panel of Fig. 7. Capture into resonance makes the eccentricities of both planets grow rapidly before they saturate at values of $e_J \sim 0.06$ and $e_o \sim 0.27$. Here again, the long-term evolution of the system appears to be inward migration with the two planets maintaining their commensurability. Moreover, this two-planet system tends ultimately to evolve to a state in which the two planets orbit within a common gap, as can be seen in the lower panel of Fig. 8 which shows a snapshot of the disc surface density at $t \sim 10^4$ orbits.

The results of this calculation are broadly consistent with previous hydrodynamical simulations of two Jovian-mass planets interacting with their protoplanetary disc (Snellgrove et al. 2001; Papaloizou 2003; Kley et al. 2005). However, the initial conditions that we employ here are different from the ones used

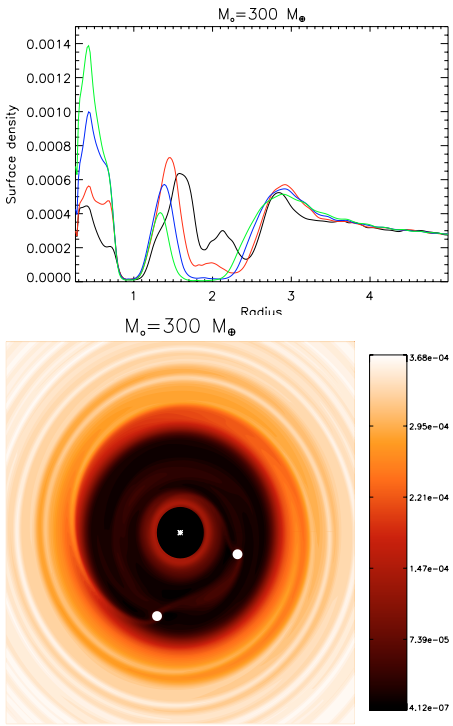

Fig. 8. *Upper panel*: this figure shows the disc surface density profile for model *R*7 at $t = 100$ (black line), 300 (red line), 600 (blue line) and 900 (green line) orbits. *Lower panel*: this figure shows in linear scale a snapshot of the disc surface density at $t \sim 10^4$ orbits for the same model. In this figure, planets are represented by white circles.

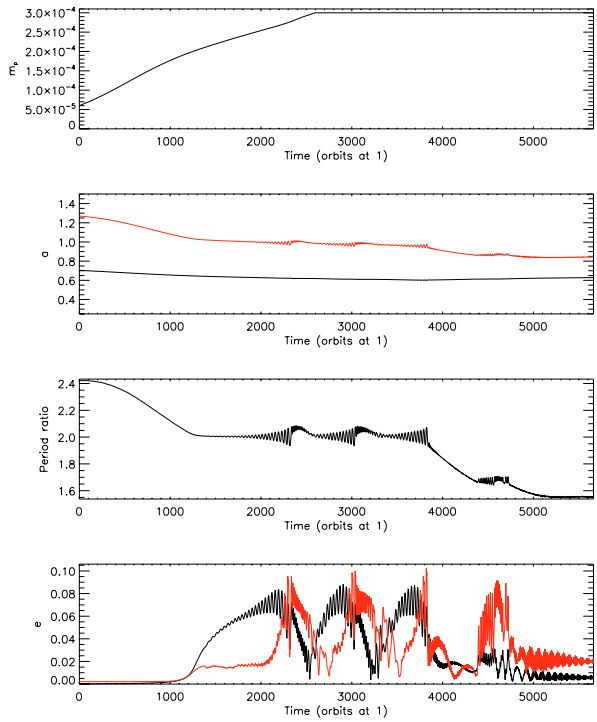

Fig. 9. Evolution of a 20 $M_\oplus$ core initially trapped at the edge of Jupiter'gap and accreting gas material from the disc. *Upper (first) panel*: this figure shows the mass of the core as a function of time. *Second panel*: this figure shows the evolution of the semi-major axes of the planets. *Third panel*: evolution of the period ratio $p = (a_o/a_J)^{3/2}$. *Lower panel*: evolution of the eccentricities of the planets.

in most of the previous studies, in which the two-planet system is assumed to initially orbit inside a cavity. This indicates that trapping into 2:1 resonance is a robust outcome of such a system.

4. Consequences for the early Jupiter-Saturn system

In this section we discuss the results of our simulations in the context of recently proposed models for the early evolution of the outer Solar System. The so-called "Nice model" (Tsiganis et al. 2005; Morbidelli et al. 2005; Gomes et al. 2005) proposes a scenario in which the outer planets were in a more compact configuration just after dissipation of the gas disc, with Saturn orbiting interior to the 2:1 mean motion resonance with Jupiter. Subsequent scattering of the exterior planetesimal disc causes the three outer planets to migrate outward, during which time Jupiter and Saturn cross their mutual 2:1 resonance. This triggers a global instability leading to the orbital structure of the outer Solar System observed today. More recent work by Morbidelli et al. (2007) shows that a similar outcome may be obtained if Jupiter and Saturn were originally in the 3:2 resonance, with a global instability being triggered when they cross the 5:3 resonance. They have shown that a model may be constructed in which all four outer Solar System planets were in mutual mean motion resonances, and for which the net disc torques acting on the planets is zero resulting in no migration of the system.

The simulations presented in this paper raise a number of questions within the context of this scenario. The most obvious one is whether it is possible for Saturn to have been in the 3:2 resonance with Jupiter prior to the onset of global instability, if it had formed further out in the disc. Our results, in agreement with those of Masset & Snellgrove (2001) and Morbidelli & Crida (2007), show that a fully formed Saturn is able to migrate into the 3:2 resonance. But they also show that a lower mass core can either be trapped at the edge of Jupiter's gap, or else be captured in the 2:1 resonance instead. It is not clear that this core, when it grows in mass, will actually migrate through and be locked in 3:2. Moreover, capture in the 2:1 resonance may depend on the disc density and examining whether or not Saturn passes through the 2:1 resonance in a less massive disc remains an outstanding issue. To investigate these questions, we have performed an additional suite of eight simulations.

In four of these simulations we initiated the system with a 20 $M_\oplus$ core trapped at the edge of Jupiter's gap. In each simulation the core is able to accrete gas from the disc. For each of the four runs we varied the accretion rate so that the time scale for the core to reach one Saturn mass ranged between 500 to 2500 initial Jovian orbital periods. Interestingly, each simulation resulted in the same final outcome, with Jupiter and Saturn locked in the 3:2 resonance. Figure 9 shows the results of a simulation in which the core grows to a Saturn mass in ~2500 orbits. Typically, the evolution of the core proceeds as follows. At the beginning of the simulation, the core leaves the edge of Jupiter's gap since as it grows, the coorbital region is depleted and corotation torques weaken. Subsequent evolution involves further growth of the core and convergent migration of the two planets until capture into 2:1 resonance. In each simulation however, the accreting core breaks free from the 2:1 resonance once its mass has reached one Saturn mass. Continuation of the runs indicate that the 5:3 resonance can be temporary established but that ultimately, Saturn becomes locked in the 3:2 resonance with Jupiter.

A fifth simulation was performed in which a 30 $M_\oplus$ core was initially located in the 2:1 resonance with Jupiter. Gas accretion was initiated onto the core such that it would reach one Saturn mass in 2500 Jovian orbits. Once again the 2:1 resonance was broken as the core approached one Saturn mass, with the planet finally settling into the 3:2 resonance.

Finally, we performed three additional simulations that study the evolution of a fully formed Saturn as a function of the disc surface density. In these three simulations, the initial surface density profile is the same as that described in Sect. 2.2, but the total disc mass is reduced by factors of 2, 4 and 8, corresponding to $M_\mathrm{d} = 10^{-2}$, 5×10^{-3} and 2.5×10^{-3} $M_\odot$, respectively. Reduction by a factor of 1/2 leads to the Saturn-mass planet passing through the 2:1 resonance, and capture in 3:2. Reduction of the disc mass by factors of 1/4 or 1/8, however, leads to a new mode of evolution. Here, the Saturn-mass planet is captured into the 2:1 resonance for approximately 3×10^3 orbits when $M_\mathrm{d} = 5 \times 10^{-3}$ $M_\odot$, and for approximately 1×10^4 orbits when $M_\mathrm{d} = 2.5 \times 10^{-3}$ $M_\odot$. The resonance then breaks in each case, and the planet is scattered outward by a small distance such that it orbits just outside of the 2:1 resonance. This configuration is maintained over runs times of 6×10^3 orbits, without any sign of recapture into the resonance, or migration through it. Analysis of the disc torques experienced by the Saturn mass planet show that they are essentially zero, apparently because a small orbital eccentricity ($e \simeq 0.08$) is maintained, leading to torque cancellation as the Saturn-mass planet orbits at the edge of the gap formed by the inner giant.

The series of simulations presented in this section suggest that trapping into the 3:2 resonance is a very robust evolutionary outcome of a Jupiter-Saturn system embedded in a protoplanetary disc, provided the disc is sufficiently massive. In this case capture of the planet into 3:2 is found to be independent of the earlier evolution of proto-Saturn. Indeed these results show that such models cannot be used to constrain in detail the formation history of Saturn prior to its supposed trapping in the 3:2 resonance with Jupiter. Three possible Saturn formation scenarios exist, and none of these can be excluded by the simulations presented in this paper: (*i*) full formation of Saturn in situ close to the 3:2 resonance followed by capture into it; (*ii*) full formation of Saturn out beyond the 2:1 resonance with Jupiter, followed by subsequent migration into the 3:2 resonance; (*iii*) formation of Saturn's core and its trapping at the edge of Jupiter's gap (or in the 2:1 resonance with Jupiter), with further growth through gas accretion causing inward migration into the 3:2 resonance. The simulations performed with significantly lower disc masses, however, indicate that capture into 3:2 would have been much less probable if Jupiter and Saturn had formed late in the life time of the solar nebula when the disc was being dispersed.

5. Conclusion

We have presented the results of hydrodynamic simulations of two planets embedded in a protoplanetary disc. The inner planet is a gas giant with a mass of 1 M_J, and the outer planet has a mass that ranges between 10 $M_\oplus$ to 1 M_J. Our simulations suggest three possible evolutionary pathways for such a system of two planets. The first involves divergent migration, which arises when the inner planet migrates inward at a faster rate than the outer planet. We estimate that this occurs when the outer planet has a mass $m_\mathrm{o} \lesssim 3.5$ $M_\oplus$. The second involves the outer planet becoming trapped at the edge of the gap formed by the interior giant, due to corotation torques, and arises for outer planet masses in the range $10 \leq m_\mathrm{o} \leq 20$ $M_\oplus$. The third involves resonant capture of the outer planet as it migrates toward the giant. For planet masses in the range $30 \leq m_\mathrm{o} \leq 40$ $M_\oplus$, and for $m_\mathrm{o} = 1$ M_J, capture is into the 2:1 resonance. For planet masses in the range $80 \leq m_\mathrm{o} \leq 100$ $M_\oplus$, capture into the 3:2 resonance occurs. These results are relevant to observations of extrasolar multiplanet systems, since they suggest that there exists a lower mass limit for the capture of an outer planet into a mean motion resonance with an interior Jovian mass body. They suggest that Neptune-mass planets and below should not be observed in resonance with an interior giant planet. Planets with mass in excess of 30 $M_\oplus$ may, however, be observed in such resonances.

We discussed the results of our simulations within the context of the early history of the outer Solar System, and presented some calculations of Saturn's core being initially trapped at the edge of Jupiter's gap (and in the 2:1 resonance) and growing through the accretion of gas from the disc. We demonstrated that the final state of the Jupiter-Saturn system is likely to be trapping in 3:2 resonance, and that such an outcome does not depend on the earlier evolution of Saturn's core. These results provide support for the idea that the outer planets were in a much more compact configuration during the early evolution of the Solar System, with Jupiter and Saturn being locked in the 3:2 resonance (Morbidelli et al. 2007).

Acknowledgements. The simulations performed in this paper were performed on the QMUL High Performance Computing facility purchased under the SRIF initiative, and on the UK Astrophysical Fluids Facility.

References

Crida, A., Morbidelli, A., & Masset, F. 2007, A&A, 461, 1173
De Val-Borro, M., Edgar, R. G., Artymowicz, P., et al. 2006, MNRAS, 370, 529
Hahn, J. M., & Ward, W. R. 1996, Lunar and Planetary Institute Conference Abstracts, 27, 479
Kley, W., Peitz, J., & Bryden, G. 2004, A&A, 414, 735
Kley, W., Lee, M. H., Murray, N., & Peale, S. J. 2005, A&A, 437, 727
Gomes, R., Levison, H. F., Tsiganis, K., & Morbidelli, A. 2005, Nature, 435, 466
Lee, M. H., & Peale, S. J. 2002, ApJ, 567, 596
Masset, F., & Snellgrove, M. 2001, MNRAS, 320, L55
Masset, F. S., & Papaloizou, J. C. B. 2003, ApJ, 588, 494
Masset, F. S., Morbidelli, A., Crida, A., & Ferreira, J. 2006, ApJ, 642, 478
Morbidelli, A., & Crida, A. 2007 [arXiv/0704.1210]
Morbidelli, A., Levison, H. F., Tsiganis, K., & Gomes, R. 2005, Nature, 435, 462
Morbidelli, A., Tsiganis, K., Crida, A., Levison, H. F., & Gomes, R. 2007, [arXiv:0706.1713]
Nelson, R. P., & Papaloizou, J. C. B. 2002, MNRAS, 333, L26
Nelson, R. P., Papaloizou, J. C. B., Masset, F., & Kley, W. 2000, MNRAS, 318, 18
Ogilvie, G. I., & Lubow, S. H. 2003, ApJ, 587, 398
Papaloizou, J. C. B. 2003, Cel. Mech. Dyn. Astron., 87, 53
Papaloizou, J. C. B., & Larwood, J. D. 2000, MNRAS, 315, 823
Papaloizou, J. C. B., & Nelson, R. P. 2005, A&A, 433, 247
Press, W. H., Teukolsky, S. A., Vetterling, W. T., & Flannery, B. P. 1992 (Cambridge: University Press), 2nd edn.
Shakura, N. I., & Sunyaev, R. A. 1973, A&A, 24, 337
Snellgrove, M. D., Papaloizou, J. C. B., & Nelson, R. P. 2001, A&A, 374, 1092
Stone, J. M., & Norman, M. L. 1992, ApJS, 80, 753
Tanaka, H., Takeuchi, T., & Ward, W. R. 2002, ApJ, 565, 1257
Thommes, E. W. 2005, ApJ, 626, 1033
Tsiganis, K., Gomes, R., Morbidelli, A., & Levison, H. F. 2005, Nature, 435, 459
Ward, W. R. 1997, Icarus, 126, 261